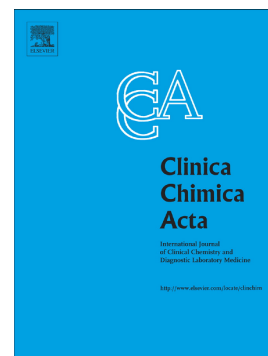


Analysis of urine cell-free DNA copy number and fragment size from healthy individuals

Jufen Wang, Zilong Wu, Bingyu Wu, Xinghao Lin, Wenhe Wu, Jun Li



PII: S0009-8981(25)00506-6  
DOI: <https://doi.org/10.1016/j.cca.2025.120627>  
Reference: CCA 120627

To appear in: *Clinica Chimica Acta*

Received date: 26 July 2025  
Revised date: 8 September 2025  
Accepted date: 21 September 2025

Please cite this article as: J. Wang, Z. Wu, B. Wu, et al., Analysis of urine cell-free DNA copy number and fragment size from healthy individuals, *Clinica Chimica Acta* (2024), <https://doi.org/10.1016/j.cca.2025.120627>

This is a PDF file of an article that has undergone enhancements after acceptance, such as the addition of a cover page and metadata, and formatting for readability, but it is not yet the definitive version of record. This version will undergo additional copyediting, typesetting and review before it is published in its final form, but we are providing this version to give early visibility of the article. Please note that, during the production process, errors may be discovered which could affect the content, and all legal disclaimers that apply to the journal pertain.

# Analysis of Urine Cell-free DNA Copy Number and Fragment Size from Healthy Individuals

Jufen Wang<sup>a,b</sup>, Zilong Wu<sup>b</sup>, Bingyu Wu<sup>b</sup>, Xinghao Lin<sup>b</sup>, Wenhe Wu<sup>b,\*</sup>, Jun Li<sup>a,b,\*</sup>

<sup>a</sup> Department of Clinical Laboratory, Wenzhou People's Hospital/Wenzhou Maternal and Child Health Care Hospital/The Third Clinical Institute Affiliated to Wenzhou Medical University, Wenzhou, Zhejiang 325035, China

<sup>b</sup> Key Laboratory of Laboratory Medicine, Ministry of Education, Wenzhou Key Laboratory of Cancer Pathogenesis and Translation, School of Laboratory Medicine and Life Sciences, Wenzhou Medical University, Wenzhou, Zhejiang 325035, China

\*Corresponding author

Email addresses: wuwenhe2000@163.com (W. Wu), lijun005034@163.com (J. Li)

## Abstract

*Objective:* This study characterizes urine cell-free DNA (cfDNA) copy number and fragment size in healthy individuals and explores their associations with routine clinical parameters.

*Methods:* Sixty healthy subjects were enrolled, providing paired blood and urine samples. Six primer pairs targeting nuclear (*GAPDH*-61/168/241) and mitochondrial DNA (*ND1*-57/167/240) were designed for absolute qPCR. Optimal urine collection, pre-treatment, and cfDNA detection protocols were evaluated. Correlations between cfDNA characteristics (fragment size and copy number) and clinical parameters

(complete blood count, urinalysis, hepatic/renal function biomarkers) were analyzed.

**Results:** Non-extracted urine retained a higher proportion of fragments <100 bp and >2000 bp than extracted samples. The optimal pre-treatment involved immediate EDTA addition, centrifugation at 4°C, and storage at -80°C. Urine cfDNA comprised short, medium, and long fragments. Cell-free mitochondrial DNA (cf-mtDNA) showed the highest copy numbers in short fragments, decreasing with length, whereas cell-free nuclear DNA (cf-nDNA) peaked in medium fragments. *NDI-57* Cq values correlated negatively with neutrophil percentage ( $P < 0.01$ ) and positively with lymphocyte percentage ( $P < 0.05$ ). Lymphocyte percentage was moderately correlated with *NDI* short fragment (*NDI-S*,  $P < 0.01$ ) and weakly with the *NDI-S* to *NDI* medium fragment (*NDI-M*) ratio ( $P < 0.05$ ). Absolute lymphocyte count correlated weakly with *NDI-S* ( $P < 0.01$ ) and *NDI-M* ( $P < 0.05$ ). Neutrophil percentage correlated weakly with *NDI-S* ( $P < 0.01$ ) and *NDI-S* to *NDI* long fragment (*NDI-L*) ratio ( $P < 0.05$ ).

**Conclusion:** Urine cfDNA displays three distinct fragment sizes, with cf-mtDNA predominantly found in short fragments and showing stronger associations with physiological parameters than cf-nDNA.

**Keywords** Urine; Cell-free mtDNA; Cell-free nDNA; Pre-treatment conditions; Biomarker

## 1. Introduction

Cell-free DNA (cfDNA), present in both plasma and urine, serves as a promising

biomarker, with its fragment size and copy number holding potential for disease screening and physiological monitoring[1]. Urine cfDNA, compared with plasma cfDNA, offers several advantages, including non-invasiveness, ease of collection, larger sample volume, reduced protein interference, and lower susceptibility to leukocyte-derived genomic DNA interference. Therefore, it is considered more suitable for cancer diagnosis, prognosis, therapeutic monitoring, and prenatal testing[2,3]. For certain tumor types or anatomical locations, analyzing tumor DNA (ctDNA) analysis from urine may provide higher sensitivity than plasma-based assays[4]. Numerous studies have demonstrated significant differences in cfDNA fragment size and copy number in the urine of patients with various disease states compared to healthy individuals[5-7]. A prognostic study on chronic kidney disease reported that lower levels of urine cell-free mitochondrial DNA(cf-mtDNA), cell-free nuclear DNA(cf-nDNA), and the plasma neutrophil gelatinase-associated lipocalin were significantly associated with favorable renal outcomes at six months[8]. In addition, quantitative cfDNA can be serve as a biomarker to reflect prognosis and evaluate the role of urine donor-derived cfDNA in allogeneic monitoring of solid organ transplant recipients[9].

Urine cfDNA primarily originates from two primary sources, based on the formation mechanisms of ctDNA in urine. The first source is renal-derived DNA from plasma, which enters the urine via glomerular filtration and typically has a small fragment size (usually <250 bp) and low concentration[4]. The second source is DNA shed directly from epithelial cells along the urinary tract, which bypasses glomerular

filtration and thus exists as larger fragments[10]. Moreover, pre-treatment factors significantly impact the fragment size and copy number of urine cfDNA[11]. During sample transportation, handling, and storage, factors such as transportation delays, temperature fluctuations, and prolonged storage can promote cfDNA degradation and contamination by leukocyte-derived genomic DNA[12]. Several studies have reported that pre-analytical variables substantially influence cfDNA detection outcomes[13-16]. Therefore, optimizing urine cfDNA collection and processing protocols is essential for accurately measuring fragment size and copy number, particularly for cancer screening and other disease-related applications.

To advance the current understanding of urine cfDNA and its physiological distribution in healthy individuals, this study was designed to establish a standardized pre-analytical workflow and to develop an efficient, cost-effective, and reliable method for assessing fragment size and copy number variations. Furthermore, we examined the potential correlations between urine cfDNA levels and routine clinical parameters, providing a biological interpretation of these associations. These efforts collectively aim to establish technical standards and a scientific basis for future cfDNA-based diagnostic applications, thereby supporting the development of predictive models for non-invasive disease screening.

## **2. Patients and methods**

### **2.1 Subject selection**

A total of sixty-five participants (aged 21-40 years; 57% male and 43% female) undergoing routine health examinations were randomly selected from outpatients undergoing routine health examinations Wenzhou People's Hospital between October and December 2023, with a mean body mass index (BMI) of 22.48 kg/m<sup>2</sup> (range: 17.2-45.5 kg/m<sup>2</sup>). The inclusion criteria were as follows: Age between 21 and 40 years. Normal physical examination findings. No history or current diagnosis of chronic diseases affecting the heart, liver, kidneys, gastrointestinal tract, respiratory system, hematological system, or nervous system. No history of malignancies or severe illness (e.g., hepatitis, cirrhosis, chronic obstructive pulmonary disease, or colorectal disease). No positive HIV or syphilis test results. No clinically significant abnormalities detected in electrocardiogram, abdominal ultrasounds, or other examinations. Blood and urine samples were collected, and complete clinical data were recorded. After excluding participants who did not meet the inclusion criteria, a final cohort of sixty eligible subjects was included in further experimental. The study was approved by the Wenzhou People's Hospital Ethics Committee (approval number: 2022-082), and all procedures were conducted in accordance with the Declaration of Helsinki.

## **2.2 Sample collection and pre-treatment steps**

Plasma samples were collected and processed in accordance with cfDNA-specific guidelines issued by the NCI Biobank and the Division of Biological Sample Research, based on established protocols. Following the recommended protocol for plasma cfDNA collection, blood samples were drawn from participants, mixed with an

anticoagulant, and centrifuged at  $1600 \times g$  for 10 minutes at  $4^{\circ}\text{C}$ . The resulting supernatant was then centrifuged again at  $16,000 \times g$  for 10 minutes at  $4^{\circ}\text{C}$ . The final supernatant was collected and stored at  $-80^{\circ}\text{C}$  until further use. Following the urine sample processing, cfDNA extraction, and preservation methods described by Markus et al.[2], urine samples were collected from participants and divided into several pre-treatment groups. The factors included EDTA addition, storage temperatures (room temperature,  $4^{\circ}\text{C}$ , or  $-80^{\circ}\text{C}$ ), and different storage durations, with the aim of identifying optimal pre-treatment conditions.

### **2.3 cfDNA extraction and determination**

cfDNA was extracted from both plasma and urine samples using the MiniMax™ High-Efficiency cfDNA Isolation Kit (Apostle, USA), following the manufacturer's rapid extraction protocol. Fragment size distribution was analyzed using the Agilent 4150 TapeStation system, in accordance with the manufacturer's instructions.

### **2.4 Pre-analysis of cfDNA by agarose gel electrophoresis**

Agarose gels were prepared with  $1 \times$  TAE buffer. After cooling, GoldView I nucleic acid stain was added, thoroughly mixed, and poured into the gel casting tray. Electrophoresis was conducted at 100 V for 30 minutes. DNA bands were visualized using the Bio-Rad GelDoc XR imaging system to determine the DNA length of non-extracted urine samples and extracted samples following PCR amplification.

### **2.5 qPCR evaluation of copy number of cf-mtDNA and cf-nDNA**

Specific primer pairs were designed to quantify cfDNA copy number across three

fragment size ranges (Fig. S1). Quantification of cf-mtDNA and cf-nDNA was performed using SYBR Green-based quantitative real-time PCR kits (Vazyme). According to the cfDNA fragment lengths reported by Chen A et al.[17], and given the high specificity and stability of the *NDI* and *GAPDH* genes, we amplified cf-mtDNA and cf-nDNA fragments using *NDI* and *GAPDH* primers. Due to the primer binding sites, the fragment start positions for *NDI* and *GAPDH* differed slightly. Therefore, we defined the fragment ranging from *NDI*-57 to *NDI*-167 as *NDI* short fragment (*NDI*-S) and the fragment spanning from *GAPDH*-61 to *GAPDH*-168 as *GAPDH* short fragment (*GAPDH*-S). Similarly, the fragment extending from *NDI*-167 to *NDI*-240 is designated as *NDI* medium fragment (*NDI*-M), and the fragment from *GAPDH*-168 to *GAPDH*-241 is designated as *GAPDH* medium fragment (*GAPDH*-M). Any fragment larger than *NDI*-240 is classified as *NDI* large fragment (*NDI*-L), and *GAPDH*-241 onward is classified as *GAPDH* large fragment (*GAPDH*-L).

## 2.6 Statistical analysis

Statistical analyses were conducted using SPSS version 22.0. Exploratory data analysis was performed to assess the normality of data distribution. For normally distributed variables, data were expressed as mean  $\pm$  standard deviation ( $\bar{x} \pm s$ ). For non-normally distributed variables, results were presented as median and interquartile range [M (Q25, Q75)]. Pearson correlation analysis was applied for normally distributed variables, while Spearman correlation analysis was used for non-normally distributed data. Statistical significance was set at  $P < 0.05$ .



### 3. Results

#### 3.1 Differences in cfDNA fragments between plasma and urine

To assess differences in cfDNA fragment sizes distributions between extracted and non-extracted cfDNA samples, we used the Agilent 4150 TapeStation to analyze both plasma and urine cfDNA (Fig. 1). Extracted and non-extracted plasma samples were also analyzed as controls to compare cfDNA fragment size distributions between urine and plasma. In the extracted plasma samples, no peaks were detected below 200 bp. However, a minor peak at 178 bp was observed in the non-extracted plasma samples (after 5-fold dilution). Similarly, no peaks below 200 bp were observed in extracted urine samples. However, a distinct peak at 62 bp was observed in the non-extracted urine samples (after 5-fold dilution). The cfDNA fragments in non-extracted urine samples were shorter than that in non-extracted plasma samples. A distinct 62 bp peak was identified in the non-extracted urine sample, whereas neither the extracted nor non-extracted plasma samples exhibited peaks below 100 bp. These findings indicate that cfDNA fragment size distributions differ between urine and plasma.

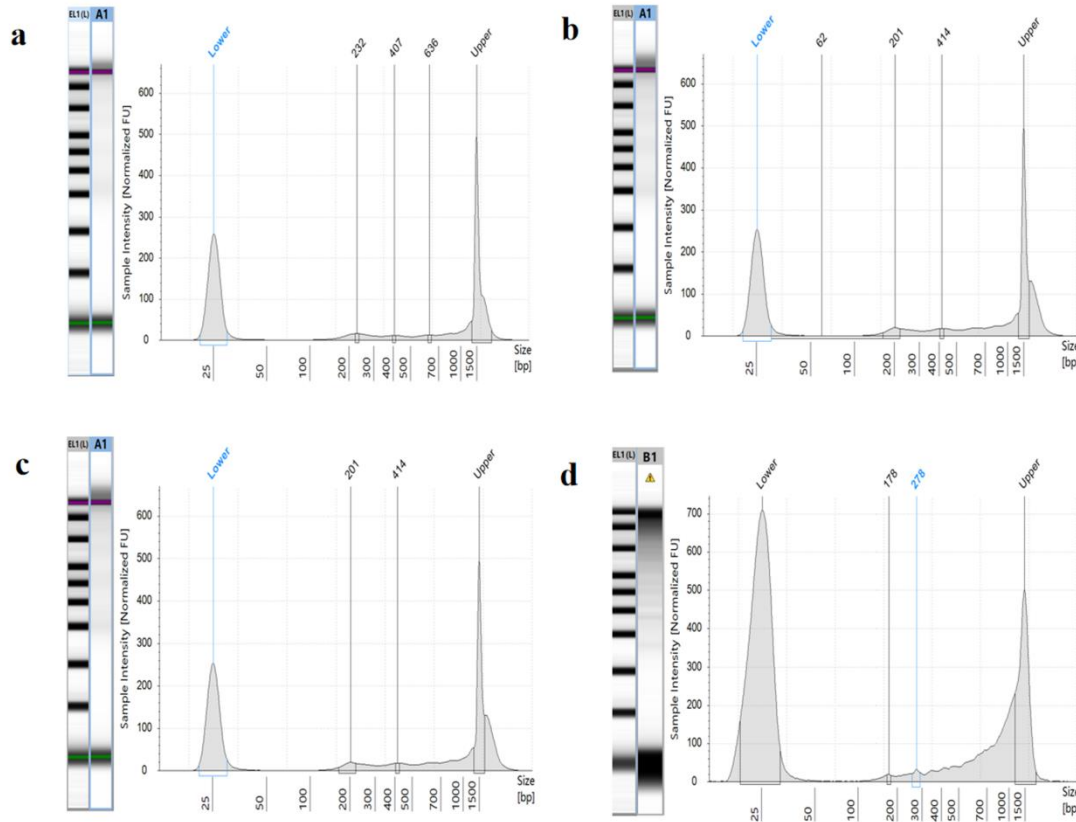


**Fig. 1. Fragment size distributions of cfDNA in urine and plasma measured by Agilent 4150 TapeStation.** a. Extracted urine samples. b. Non-extracted urine samples (after 5-fold dilution). c. Extracted plasma samples. d. Non-extracted samples (after 5-fold dilution).

### 3.2 Extracted urine samples lost shorter and longer cfDNA fragments

To enable more intuitive verification, cfDNA fragments were ligated and amplified by PCR to assess differences in fragment size between extracted and non-extracted urine samples. Non-amplified samples exhibited minimal or no visible cfDNA bands due to low cfDNA concentrations, whereas PCR-amplified samples displayed distinct bands. After ligation and PCR, the fragment size distribution of cfDNA in both extracted and non-extracted urine samples ranged from dozen to thousand base pairs (Fig. 2). Specifically, cfDNA fragments in the non-extracted urine sample were fully illuminated, whereas those in the extracted urine sample were predominantly

distributed between 100-2000 bp. The difference shown in Fig.1 and Fig.2 suggests that both cfDNA fragments shorter than 100 bp and longer than 2000 bp may have been lost during the extraction process. Therefore, non-extracted urine samples were used in subsequent experiments to preserve the full fragment size spectrum.

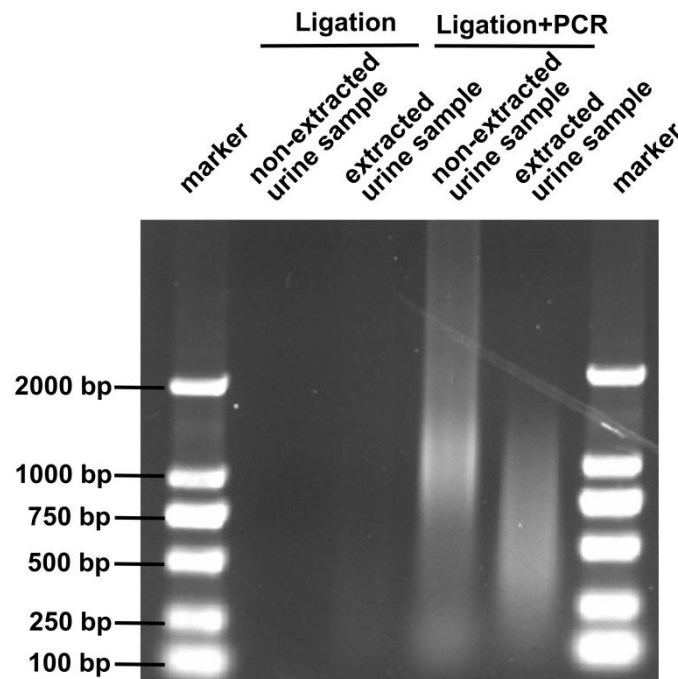


**Fig. 2. Fragment size distribution of cfDNA from both extracted and non-extracted urine samples was analyzed by agarose gel electrophoresis.** PCR amplified products displayed more uniform bands, with noticeable differences in fragment sizes between the extracted and non-extracted samples.

### 3.3 Pre-treatment conditions affect the fragment size and copy number of cfDNA in urine

Considering the variability in time intervals between urine collection and centrifugation in clinical settings, we aimed to evaluate the effects of storage temperature and EDTA addition on cfDNA integrity in non-extracted urine samples, to determine optimal pre-treatment conditions. Non-extracted urine samples were grouped

into multiple experimental conditions based on EDTA addition, storage temperature, and storage duration, with all other variables controlled. Absolute quantitative PCR (qPCR) was used to quantify cfDNA in non-extracted urine samples. Statistical analysis of the resulting Cq values was performed to identify optimal pre-treatment conditions for clinical-grade cfDNA preservation (Tables S1-S6). A standard curve for absolute quantification via PCR was generated (Fig. S1). The results demonstrated that storage at 4°C, EDTA addition, and immediate freezing of the supernatant at -80°C after centrifugation significantly influenced cfDNA fragment size and copy number. Based on these findings, the following pre-treatment conditions were applied in subsequent experiments: EDTA was added immediately after urine collection, followed by two centrifugation rounds at 4°C, and immediate freezing of the supernatant at -80°C. Frozen aliquots were thawed once for analysis, avoiding repeated freeze-thaw cycles.

### **3.4 Fragment size and copy number of cf-mtDNA and cf-nDNA in urine from healthy subjects**

Routine urine and blood test results are summarized in Tables S7-S10. The sizes and copy number of cfDNA fragments in non-extracted urine samples were measured. The variation in Cq values between replicates was less than 0.5 cycles (Tables S11, 12). Outliers ( $>0.5 \Delta Cq$ ) were excluded to ensure data consistency. Six primer pairs were used to detect three distinct fragment sizes of both cf-mtDNA and cf-nDNA, which confirmed the presence of *NDI-S* and *GAPDH-S*, *NDI-M* and *GAPDH-M*, as well as *NDI-L* and *GAPDH-L* in urine samples. Based on qPCR amplification results, the

concentration of cf-nDNA detected in urine samples was relatively low (Tables S11-S12). For copy number analysis, sixty valid *NDI* amplifications and twenty-nine *GAPDH* amplifications were selected, in which long, medium, and short fragments were successfully amplified with Cq values <35. The median (interquartile range) values for *NDI*-L/M/S were 66.16 (26.08, 93.33), 248.62 (99.50, 283.43), and 797.62 (477.59, 1067.25) copies/ $\mu$ L, respectively. For *GAPDH*-L/M/S, the median values were 4.41 (2.91, 4.41), 15.53 (7.24, 15.16), and 6.32 (2.47, 6.13) copies/ $\mu$ L, respectively. The mean copy number of *NDI*-L/M/S were 94.84, 288.11, and 1084.98 copies/ $\mu$ L, respectively. For *GAPDH*-L/M/S, the median values were 4.46, 15.53, and 6.32 copies/ $\mu$ L, respectively. Overall, the mean copy number of *NDI* fragments was consistently higher than that of corresponding *GAPDH* fragments (Fig. 3). Notably, the copy number of *NDI* fragments increased inversely with fragment size, showing the highest abundance in short fragments, followed by medium and long fragments. In contrast, *GAPDH* showed the highest copy number in medium fragments.

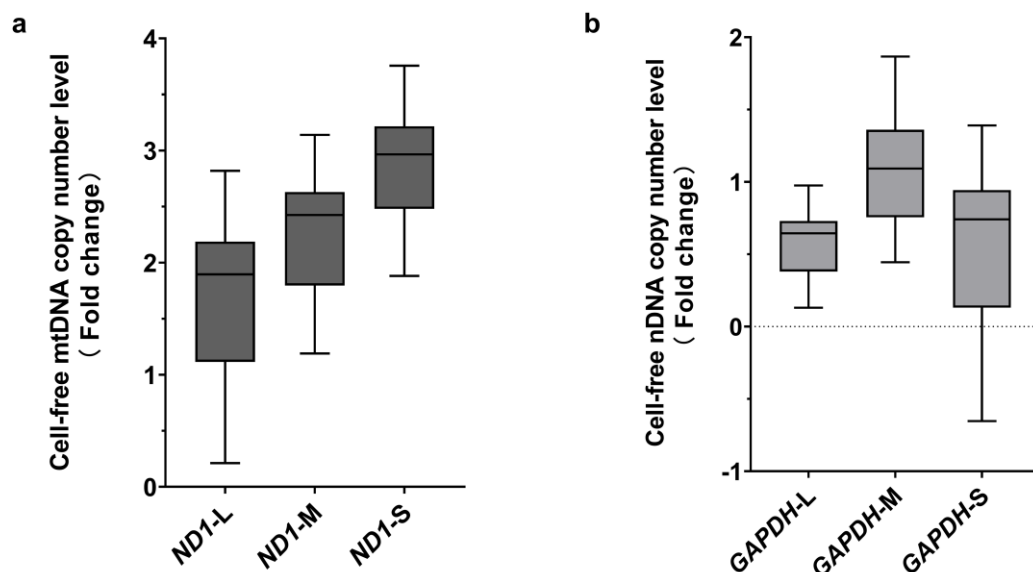


**Fig. 3. Copy number analysis was performed on short, medium, and long fragments of cf-mtDNA and cf-nDNA.** Data were derived from qPCR-amplified *NDI* (a,  $n = 60$ ) and *GAPDH* (b,  $n = 29$ ) samples. Copy number values were  $\log_{10}$ -transformed to approximate a normal distribution, meeting the assumptions of parametric statistical tests.

### **3.5 Correlation analysis between urine cfDNA characteristics and routine clinical parameters in healthy subjects**

Correlation analysis was performed between urine cfDNA fragment size/copy number and routine clinical parameters (complete blood count, urinalysis, hepatic/renal function biomarkers) in healthy subjects. Initial analysis revealed no significant associations involving *GAPDH*. Therefore, only *NDI* data were included in subsequent analyses. Pearson correlation analysis was applied to normally distributed continuous variables (Table 1), while Spearman correlation analysis was used for non-normally distributed variables (Tables 2-3). The lymphocyte percentage showed a moderate positive correlation with *NDI*-S copy number ( $r=0.391$ ,  $P=0.002$ ) and weak positive correlations with *NDI*-57 copy number ( $r=0.258$ ,  $P=0.047$ ) and the *NDI*-S/*NDI*-M ratio ( $r=0.321$ ,  $P=0.012$ ). The absolute lymphocyte count demonstrated weak positive correlations with *NDI*-57 Cq values ( $r=0.364$ ,  $P=0.004$ ) and *NDI*-167 Cq values ( $r=0.315$ ,  $P=0.014$ ), but weak negative correlations with *NDI*-57 copy number ( $r=-0.397$ ,  $P=0.002$ ), *NDI*-S ( $r=-0.388$ ,  $P=0.002$ ), and *NDI*-M ( $r=-0.306$ ,  $P=0.017$ ). Neutrophil percentage showed a weak positive correlation with *NDI*-57 copy number ( $r=0.351$ ,  $P=0.006$ ), *NDI*-S ( $r=0.397$ ,  $P=0.002$ ), and the *NDI*-S/*NDI*-L ratio ( $r=0.314$ ,  $P=0.015$ ), while it was weakly negatively correlated with the *NDI*-S/*NDI*-M ratio ( $r=-0.368$ ,  $P=0.004$ ). Urine specific gravity showed weak negative correlations with *NDI*-

57 copy number ( $r=-0.256$ ,  $P=0.048$ ) and *NDI-167* copy number ( $r=-0.317$ ,  $P=0.013$ ).

Urine pH demonstrated weak positive correlations with *NDI-57* copy number ( $r=0.258$ ,  $P=0.047$ ) and *NDI-167* copy number ( $r=0.262$ ,  $P=0.043$ ). These associations suggest that urine cf-mtDNA fragmentation may be partially shaped by immune responses and renal epithelial activity, linking systemic leukocyte dynamics to local shedding processes. Establishing these baseline urine cfDNA profiles in healthy individuals provides an essential reference for future comparative studies, including early cancer detection, renal disease monitoring, and infection-related pattern recognition.

**Table 1 Pearson correlation analysis results**

Indicators	Test	Pearson correlation coefficient	<i>P</i>
Neutrophil percentage	<i>NDI-57</i> Cq values	-0.344	0.007
Lymphocyte percentage	<i>NDI-57</i> Cq values	0.391	0.002

**Table 2 Spearman correlation analysis positive correlation results**

Indicators	Test	Spearman correlation coefficient	<i>P</i>
Absolute value of lymphocytes	<i>NDI-57</i> Cq values	0.364	0.004
Absolute value of lymphocytes	<i>NDI-167</i> Cq values	0.315	0.014
PH value	<i>NDI-57</i> copy number	0.258	0.047
Neutrophil percentage	<i>NDI-57</i> copy number	0.351	0.006
PH value	<i>NDI-167</i> copy number	0.262	0.043

Neutrophil percentage	<i>NDI-S</i>	0.397	0.002
Lymphocyte percentage	<i>NDI-S</i> to <i>NDI-M</i> ratio	0.321	0.012
Neutrophil percentage	<i>NDI-S</i> to <i>NDI-L</i> ratio	0.314	0.015

**Table 3 Spearman correlation analysis negative correlation results**

Indicators	Test	Spearman correlation coefficient	<i>P</i>
Urine Specific Gravity	<i>NDI-57</i> copy number	-0.256	0.048
Absolute value of lymphocytes	<i>NDI-57</i> copy number	-0.397	0.002
Lymphocyte percentage	<i>NDI-57</i> copy number	-0.410	0.001
Absolute value of lymphocytes	<i>NDI-167</i> copy number	-0.317	0.013
Lymphocyte percentage	<i>NDI-S</i>	-0.345	0.001
Absolute value of lymphocytes	<i>NDI-S</i>	-0.388	0.002
Absolute value of lymphocytes	<i>NDI-M</i>	-0.306	0.017
Neutrophils percentage	<i>NDI-S</i> to <i>NDI-M</i> ratio	-0.368	0.004

#### 4. Discussion

This study offers the first comprehensive characterization of urine cf-mtDNA and cf-nDNA fragment size distribution and copy number in healthy individuals using a cost-effective absolute quantitative PCR method. Our findings confirm that different pre-analytical conditions can significantly impact cfDNA yield and detection, with



increased levels potentially attributable to genomic DNA contamination during extended processing delays[18,19]. Consistent with plasma cfDNA guidelines recommending processing within two hours of blood collection into EDTA-containing tubes[20,21], we adapted plasma cfDNA-specific guidelines (developed by the Biospecimen Research Branch of the National Cancer Institute) to analyze cfDNA fragment size and copy number in non-extracted urine samples from healthy subjects, and integrated physiological characteristics into a comprehensive analysis[22].

A key finding was the significantly higher copy number of urine cf-mtDNA compared to cf-nDNA, highlighting its technical suitability as a biomarker. This may reflect either genuine biological abundance or qPCR sensitivity limitations for low-concentration cf-nDNA. Additionally, three distinct fragment sizes of urine cf-DNA (short, medium, long) were identified, consistent with our previous observations in blood and cerebrospinal fluid[17]. For cf-mtDNA, copy number decreased with increasing fragment length, with short fragments showing the highest abundance. In contrast, cf-nDNA concentration peaked in medium fragments. Conversely, cf-nDNA concentration peaked within the medium fragment range. This distinct fragmentation pattern likely stems from fundamental biological differences: short cf-mtDNA fragments dominate due to mitochondrial membrane vulnerability and rapid enzymatic degradation, while cf-nDNA's mid-size peak corresponds to DNA protected by nucleosomes during programmed cell death[23,24]. The abundance of short mitochondrial fragments offers practical advantages for detection in liquid biopsies,

whereas nuclear DNA fragments typically reflect chromatin integrity[25-27]. These size-specific signatures hold promise as indicators of tissue-specific damage mechanisms where mitochondrial patterns potentially signaling acute stressors like inflammation, and nucleosomal patterns associated with conditions like cancer[28-30].

Beyond highlighting the fragmentation differences between cf-mtDNA and cf-nDNA, our results can be contextualized within the broader exploration of urinary biomarkers. Previous studies have attempted to utilize molecular pathways such as urine miRNA, volatile metabolites, and protein/peptide features for non-invasive detection, particularly in urological oncology where alternative detection strategies have been developed[31-34]. Although these methods have different molecular sources and analysis platforms, they all point to the diagnostic potential of urine as a convenient biological fluid[35]. The combination of cfDNA fragment omics with the existing patterns highlights its translational value: short cf-mtDNA fragments can serve as rapid cellular stress indicators, while nucleosome protected cf-nDNA or non DNA molecules provide stable signals. Through this cross-modal perspective, urine cfDNA is no longer an isolated single biomarker, but an important component of a multimodal urine diagnostic system, providing more accurate application prospects for tumor monitoring, kidney disease assessment, and population screening.

We further investigated correlations between urine cf-mtDNA levels and routine clinical parameters. The neutrophil percentage (a recognized indicator of bacterial infections) showed a negative correlation with the *NDI-S* to *NDI-M* ratio and a positive

correlation with the *NDI-S* to *NDI-L* ratio. This pattern is consistent with the immune pathway, in which short mtDNA fragments released from activated neutrophils enter the urine via glomerular filtration, correlating with peripheral neutrophil consumption during inflammation[36,37]. Similarly, both lymphocyte percentage and absolute count both demonstrated negative correlations with cf-mtDNA copy numbers, potentially indicating inflammatory involvement[37]. Moreover, variations in urine specific gravity and pH not only may affect qPCR accuracy but also reflect microenvironmental modulation of mtDNA release and stability-highlighting the renal epithelial pathway, whereby cellular stress or damage leads to mitochondrial shedding via exosomes, apoptosis, or necrosis[38-40]. Collectively, these clinical and molecular associations underscore position the utility of urine cf-mtDNA as a promising non-invasive biomarker reflective of both immune activity and renal epithelial status[41,42].

This study's limitations include potential lifestyle confounders in unprocessed urine samples and ionic interference with qPCR accuracy, compounded by single-center recruitment and restricted age range (21-40 years) that limit generalizability. The cross-sectional design precludes temporal assessment, while absent disease cohorts constrain clinical relevance. Yet these baseline urine cfDNA profiles provide a robust reference for future disease-oriented investigations and enable the development of machine learning – based multimodal diagnostic models that integrate cfDNA with additional physiological indicators, thereby enhancing diagnostic accuracy and facilitating population-level screening across diverse pathologies.

## 5. Conclusion

Urine cfDNA in healthy individuals exhibited three distinct fragment sizes (short, medium, long), with cf-mtDNA abundance inversely proportional to length (peaking in short fragments) while cf-nDNA peaked at medium sizes. Notably, urine cf-mtDNA shows a stronger correlation among fragment size, copy number, and clinical indicators than cf-nDNA, underscoring its superior potential as a non-invasive screening biomarker for providing functional insights into individual health status.

## CRedit authorship contributions

Study concept and design: Jufen Wang, Jun Li. Data acquisition: Bingyu Wu, Xinghao Lin. Data analysis: Jufen Wang. Drafting of manuscript: Zilong Wu, Jufen Wang. Critical revision of the manuscript: Wenhe Wu, Zilong Wu.

## Funding information

This work was supported by the Zhejiang Provincial Natural Science Foundation of China (Grant number LY23H090007), the Medical Health Science and Technology Project of Zhejiang Provincial Health Commission (Grant number 2023KY885), the Basic Project of Wenzhou Municipal Science and Technology Bureau (Grant number Y20220048, Y20220122), and Zhejiang Students' Technology and Innovation Program (Grant number 2023R413053).

## Declaration of Competing Interest

We declare that we have no financial and personal relationships with other people or organizations that can inappropriately influence our work, and there is no professional or other personal interest of any nature or kind in any product, service and/or company that could be construed as influencing the position presented in, or the review of, the manuscript entitled.

## Data availability

Data will be made available on request.

## References

- [1] AK Kim, JP Hamilton, SY Lin, Urine DNA biomarkers for hepatocellular carcinoma screening. *Br J Cancer*. 126(2022)1432-1438.
- [2] H Markus, J Zhao, T Contente-Cuomo, 2021. Analysis of recurrently protected genomic regions in cell-free DNA found in urine. *Sci Transl Med*. 13, eaaz3088.
- [3] M Sorbini, T Carradori, GM Togliatto, Technical Advances in Circulating Cell-Free DNA Detection and Analysis for Personalized Medicine in Patients' Care. *Biomolecules*. 14(2024)498.
- [4] A Tivey, M Church, D Rothwell, Circulating tumour DNA - looking beyond the blood. *Nat Rev Clin Oncol*. 19(2022)600-612.
- [5] PV Nuzzo, JE Berchuck, K Korthauer, Detection of renal cell carcinoma using plasma and urine cell-free DNA methylomes. *Nat Med*. 26(2020)1041-1043.
- [6] Y van der Pol, NA Tanyo, 2023. N Evander, Real-time analysis of the cancer genome and fragmentome from plasma and urine cell-free DNA using nanopore sequencing. *EMBO Mol Med*. 15, e17282.
- [7] S Lin, S Wang, B Xu Fragmentation patterns of cell-free DNA and somatic mutations in the urine of metastatic breast cancer patients. *J Cancer Res Ther*. 20(2024)563-569.
- [8] CC Chang, PF Chiu, CL Wu, Urinary cell-free mitochondrial and nuclear deoxyribonucleic acid correlates with the prognosis of chronic kidney diseases. *BMC Nephrol*. 20(2019)391.

- [9] C Cao, L Yuan, Y Wang, Analysis of the primary factors influencing donor derived cell-free DNA testing in kidney transplantation. *Front Immunol.* 15(2024)1435578.
- [10] EA Green, R Li, L Albiges, Clinical Utility of Cell-free and Circulating Tumor DNA in Kidney and Bladder Cancer: A Critical Review of Current Literature. *Eur Urol Oncol.* 4(2021)893-903.
- [11] AK Kim, SY Lin, Z Wang, Impact of Cell-Debris and Room-Temperature Storage on Urine Circulating Tumor DNA from Hepatocellular Carcinoma. *J Mol Diagn.* 25(2023)913-920.
- [12] P Song, LR Wu, YH Yan, Limitations and opportunities of technologies for the analysis of cell-free DNA in cancer diagnostics. *Nat Biomed Eng.* 6(2022)232-245.
- [13] IM Diaz, A Nocon, SAE Held, Pre-Analytical Evaluation of Streck Cell-Free DNA Blood Collection Tubes for Liquid Profiling in Oncology. *Diagnostics (Basel).* 13(2023)1288.
- [14] T Ruppert, A Roth, J Kollmeier, 2023. Cell-free DNA extraction from urine of lung cancer patients and healthy individuals: Evaluation of a simple method using sample volume up-scaling. *J Clin Lab Anal.* 37, e24984.
- [15] B Salfer, D Havo, S Kuppinger, Evaluating Pre-Analytical Variables for Saliva Cell-Free DNA Liquid Biopsy. *Diagnostics (Basel).* 13(2023)1665.
- [16] D Andersson, H Kristiansson, M Luna Santamaría, Evaluation of automatic cell free DNA extraction metrics using different blood collection tubes. *Sci Rep.* 15(2025)19364.
- [17] A Chen, J Li, L Wang, 2020. Comparison of paired cerebrospinal fluid and serum cell-free mitochondrial and nuclear DNA with copy number and fragment length. *J Clin Lab Anal.* 34, e23238.
- [18] S El Messaoudi, F Rolet, F Mouliere, Circulating cell free DNA: Preanalytical considerations. *Clin Chim Acta.* 424(2013)222-230.
- [19] AJ Bronkhorst, J Aucamp, PJ Pretorius Cell-free DNA: Preanalytical variables. *Clin Chim Acta.* 450(2015)243-253.
- [20] X Xue, MD Teare, I Holen, Optimizing the yield and utility of circulating cell-free DNA from plasma and serum. *Clin Chim Acta.* 404(2009)100-104.
- [21] E Henao Diaz, J Yachnin, H Grönberg, 2016. The In Vitro Stability of Circulating Tumour DNA. *PLoS One.* 11, e0168153.
- [22] SR Greytak, KB Engel, S Parpart-Li, Harmonizing Cell-Free DNA Collection and Processing Practices through Evidence-Based Guidance. *Clin Cancer Res.* 26(2020)3104-3109.
- [23] G Tsirka, A Zikopoulos, K Papageorgiou, The Ratio of cf-mtDNA vs. cf-nDNA in the Follicular Fluid of Women Undergoing IVF Is Positively Correlated with Age. *Genes (Basel).* 14(2023)1504.
- [24] MM Melamud, VN Buneva, EA Ermakov Circulating Cell-Free DNA Levels in Psychiatric Diseases: A Systematic Review and Meta-Analysis. *Int J Mol Sci.* 24(2023)3402.

- [25] M Szilágyi, O Pös, É Márton, Circulating Cell-Free Nucleic Acids: Main Characteristics and Clinical Application. *Int J Mol Sci.* 21(2020)6827.
- [26] H Wang, X Shan, M Ren, Nucleosomes enter cells by clathrin- and caveolin-dependent endocytosis. *Nucleic Acids Res.* 49(2021)12306-12319.
- [27] Y van der Pol, N Moldovan, J Ramaker, The landscape of cell-free mitochondrial DNA in liquid biopsy for cancer detection. *Genome Biol.* 24(2023)229.
- [28] N Morisi, GM Virzi, M Ferrarini, Exploring the Role of Cell-Free Nucleic Acids and Peritoneal Dialysis: A Narrative Review. *Genes (Basel).* 15(2024)553.
- [29] M Zhou, H Zhang, X Xu, 2024. Association between circulating cell-free mitochondrial DNA and inflammation factors in noninfectious diseases: A systematic review. *PLoS One.* 19, e0289338.
- [30] KE Stanley, T Jatsenko, S Tuveri, Cell type signatures in cell-free DNA fragmentation profiles reveal disease biology. *Nat Commun.* 15(2024)2220.
- [31] M Aftab, SS Poojary, V Seshan, Urine miRNA signature as a potential non-invasive diagnostic and prognostic biomarker in cervical cancer. *Sci Rep.* 11(2021)10323.
- [32] Y Hu, Z Niu, C Cao, Volatile organic compounds (VOC) metabolites in urine are associated with increased systemic inflammation levels, and smokers are identified as a vulnerable population. *Ecotoxicol Environ Saf.* 288(2024)117398.
- [33] A Hanžek, C Siatka, AE Duc Diagnostic role of urine human epididymis protein 4 in ovarian cancer. *Biochem Med (Zagreb).* 34(2024)030502.
- [34] T Lima, JE Rodrigues, B Manadas, A peptide-centric approach to analyse quantitative proteomics data- an application to prostate cancer biomarker discovery. *J Proteomics.* 272(2023)104774.
- [35] F Trindade, AS Barros, J Silva, Mining the Biomarker Potential of the Urine Peptidome: From Amino Acids Properties to Proteases. *Int J Mol Sci.* 22(2021)5940.
- [36] K Krivošíková, N Šupčíková, A Gaál Kovalčíková, Neutrophil extracellular traps in urinary tract infection. *Front Pediatr.* 11(2023)1154139.
- [37] CA Puyo, A Earhart, N Staten, Mitochondrial DNA induces Foley catheter related bladder inflammation via Toll-like receptor 9 activation. *Sci Rep.* 8(2018)6377.
- [38] Y Huang, J Chi, F Wei, Mitochondrial DNA: A New Predictor of Diabetic Kidney Disease. *Int J Endocrinol.* 2020(2020)3650937.
- [39] K Zhou, Y Liu, Q Yuan, Next-Generation Sequencing-Based Analysis of Urine Cell-Free mtDNA Reveals Aberrant Fragmentation and Mutation Profile in Cancer Patients. *Clin Chem.* 68(2022)561-573.
- [40] K Sharma, B Karl, AV Mathew, Metabolomics reveals signature of mitochondrial dysfunction in diabetic kidney disease. *J Am Soc Nephrol.* 24(2013)1901-1912.
- [41] JE Till, NJ Seewald, Z Yazdani, Corticosteroid-Dependent Association between Prognostic Peripheral Blood Cell-Free DNA Levels and Neutrophil-Mediated NETosis in Patients with Glioblastoma. *Clin Cancer Res.* 31(2025)1292-1304.

[42] R Hammad, M Eldosoky, SH Fouad, Circulating cell-free DNA, peripheral lymphocyte subsets alterations and neutrophil lymphocyte ratio in assessment of COVID-19 severity. *Innate Immun.* 27(2021)240-250.



### Highlights

1. Urinary cfDNA exhibits short, medium, and long fragment sizes.
2. cf-mtDNA peaks in short fragments, cf-nDNA peaks in medium fragments.
3. cf-mtDNA shows stronger clinical relevance.